RadioGraphics

In Vivo Proton MR Spectroscopy of the Breast[1]

Peter Stanwell, PhD • Carolyn Mountford, DPhil

TEACHING POINTS
See last page

In vivo proton magnetic resonance (MR) spectroscopy (hydrogen 1 spectroscopy) provides useful information about the pathology of breast lesions by the measurement of diagnostic chemicals visible on the MR timescale. Spectroscopic measurements may be obtained following contrast-enhanced MR imaging by applying a point-resolved spatially localized spectroscopy sequence. The observation of resonances at discrete spectral frequencies allows an accurate diagnosis. In spectra obtained in vivo in malignant breast cancers, an observed resonance at 3.23 ppm is consistent with phosphocholine. In spectra from benign breast lesions and some normal breast tissue in lactating mothers and in some nonlactating healthy women, a recorded resonance at 3.28 ppm is thought to originate from glycerophosphocholine, taurine, or myoinositol. The success of in vivo spectroscopy depends on the appropriate pre-acquisition setup, acquisition protocol, and postprocessing techniques for achieving high spectral resolution and a signal-to-noise ratio sufficient to separate the resonances of the important biomarkers. When implemented correctly, the method is diagnostically accurate and robust.
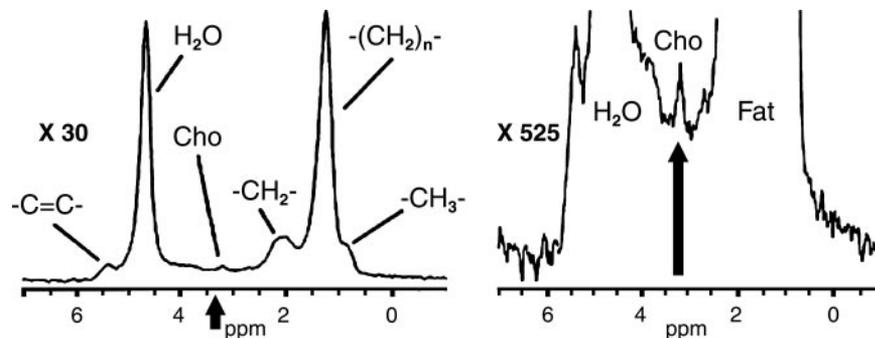
©RSNA, 2007

Figure 1. Proton single-voxel spectra obtained by using the STEAM sequence (repetition time [TR] = 2000 msec, echo time [TE] = 31 msec) at 1.5 T in a breast cancer patient. The spectrum on the left shows strong water and lipid signals, and the total choline resonance (arrow) is visible at 3.2 ppm. On the right, the vertical display is increased by 525 times, whereupon the choline resonance is now more apparent. (Reprinted, with permission, from reference 13.)

Introduction

Presurgical assessment of the pathologic type, spatial location, and extent of breast lesions has the potential to greatly improve the management of breast cancer. Contrast-enhanced magnetic resonance (MR) imaging has gained acceptance as an important breast imaging modality but does not always lead to a definitive diagnosis. In March 2007, it was reported that MR imaging could improve the diagnostic accuracy of clinical breast examination and mammography by enabling the detection of contralateral breast cancer soon after the initial diagnosis of unilateral breast cancer. Investigators in a multi-institutional and multinational study had found that the specificity of MR imaging in their patient cohort was 88% (1).

Soon afterward, a report from the American Cancer Society suggested guidelines for screening with the use of MR imaging as an adjunct to mammography (2). The following statement appears in these guidelines: "MR imaging scans are more sensitive than mammograms, but they are also more likely to show spots in the breast that may or may not be cancer. Often there is no way of knowing whether or not these spots are cancerous short of a follow-up biopsy or some other invasive procedure."

These comments give rise to the question of whether the diagnostic accuracy of breast MR imaging can be improved with the adjunctive use of in vivo proton MR spectroscopy (hydrogen 1 [^{1}H] spectroscopy). A current goal therefore is the further development of in vivo proton MR spectroscopy to enable an accurate and reliable preoperative diagnosis of breast lesions. This is an area of active research in several laboratories worldwide.

The chemistry of human tissues and organs is altered in the presence of disease, and these changes in cellular chemistry are measurable with ^{1}H MR spectroscopy (3,4). ^{1}H MR spectroscopy of fine-needle aspiration biopsy specimens from the breast provides a wealth of diagnostic and prognostic information (5,6). How much of this useful information can be obtained with in vivo spectroscopy remains to be determined.

Choline-containing compounds have been identified as biomarkers of cancer (7–10). The results of ex vivo studies have shown that the choline resonance present in breast cancer tissue is a composite produced by signals from several biochemicals (11,12). The primary constituents include free choline, phosphocholine, and glycerophosphocholine; in addition, taurine, glucose, phosphoethanolamine, and myoinositol may contribute to the composite resonance (12). Recent evidence indicates that the appearance of phosphocholine in the spectrum is due mainly to increased choline kinase activity and increased catabolism mediated by increased phospholipase C activity (8).

The individual resonances that are clearly resolved in ex vivo studies are broadened in the in vivo MR spectra, and they coalesce into a broadened composite resonance. The initial report about the application of in vivo MR spectroscopy in the breast was published by Roebuck and colleagues, who found a choline resonance at 3.2 ppm in spectra from cancerous tissues (13). They also found that in some individuals a strong lipid (fat) signal might mask a potentially diagnostic choline resonance (Fig 1). The results of a later series of studies of breast MR spectroscopy in vivo at 1.5–4.0 T with a range of surface coils and pulse sequences have been summarized in several publications (9,14). A number of authors have proposed that the broad composite resonance at
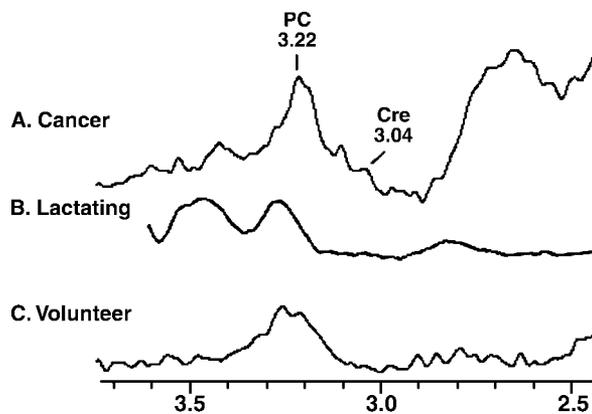
Figure 2. Typical 1.5-T proton single-voxel spectra obtained by using the PRESS sequence (TR = 2000 msec, TE = 135 msec; 256 signals acquired). Data were acquired by using a commercially available MR imaging system (GE Healthcare, Milwaukee, Wis) and a specially designed double breast coil (23). After acquisition, the data were zero-filled from 2048 to 8192 data points, and a Gaussian apodization function of 1.5 Hz with a 15% echo offset was applied before fast Fourier transform. The spectra were referenced to the methylene resonance of lipid at 1.33 ppm and water at 4.74 ppm. In the spectral region shown (2.5–3.7 ppm), the following may be evident: creatine-containing compounds at 3.04 ppm; phosphocholine at 3.22 ppm; and glycerophosphocholine, taurine, and myoinositol, which coresonate at 3.28–3.35 ppm. *A,* Patient with histologically confirmed invasive ductal carcinoma. *B,* Lactating volunteer (voxel collected from glandular tissue). *C,* Nonlactating volunteer (voxel collected from glandular tissue). In the spectrum from the cancer patient, resonances can be assigned to creatine-containing compounds *(Cre)* (3.04 ppm) and phosphocholine *(PC)* (3.22 ppm). In the spectra from the lactating and nonlactating volunteers, spectral referencing reveals a different chemical shift for the center of the tCho resonance, which is at 3.28 ppm. This shift may be due to a different chemical species (glycerophosphocholine, taurine, or myoinositol or a combination thereof) as yet undesignated. (Reprinted, with permission, from reference 20.)

3.2 ppm, produced by choline and choline-containing compounds and denoted as total choline-containing compounds (tCho), be considered a stand-alone marker of malignant disease (9,15–19). However, that hypothesis is disputable; the present authors (20) and others (21,22) have questioned the validity of using the simple detection of such a broad composite resonance as a marker for malignancy. However, at the higher magnetic field strength of 4.0 T, the intensity of the choline resonance measured in volunteer (control) subjects is such that quantification of the tCho signal has been advocated as a possible means of diagnosing malignancy (21).

Using a custom-built surface coil and carefully implemented experimental protocols (23), at the lower magnetic field strength of 1.5 T, it was found that the center of the composite choline resonance is at a different spectral frequency in malignant cancer than in normal breast tissue. It also was found that the composite choline resonance in some instances could be resolved into multiple resonances (20). Spectra from invasive breast disease showed a resonance centered at 3.23 ppm, whereas in the spectra obtained from breast tissue in healthy volunteers (including lactating mothers) the resonance was centered at 3.28 ppm (Fig 2). The assignment of the 3.28 ppm resonance remains unresolved, but likely candidates are taurine, glycerophosphocholine, and myoinositol. Thus, the term *total choline* is a misnomer when the resonance is at 3.28 ppm.

With the increased interest in molecular imaging, there is a strong drive in the research community to use in vivo proton MR spectroscopy to help improve diagnostic specificity and prognostic capability by accurately identifying the pathologic process and to monitor the response to therapy (24–28). With the recognition that a broad resonance at 3.2 ppm is detectable in spectra from some normal glandular breast tissue, there is an increased emphasis on proficiency in the acquisition of in vivo MR spectra.

This article describes a method for obtaining in vivo MR spectra from the breast, in as short a time as possible, with a signal-to-noise ratio (SNR) sufficient to allow the diagnostic resonances to be recorded, while maintaining the highest possible spectral resolution. Success depends greatly on the capability of the MR imaging system to operate as a spectrometer.

The parameters that characterize each MR resonance include frequency, height, line width at half-height, and signal phase (which may be altered when multiple-pulse spatial localization sequences are used) (29). The frequency at which a particular proton resonates depends on the local chemical environment of that proton. Protons are influenced not only by the nuclei to which they are directly attached but also by nuclei that are nearby (both those that are spatially proximate and those that are one or two chemical bond lengths away). The height (the maximum resonance intensity) and the area under the resonance curve (the integral) may be calculated to obtain relative measurements of the concentration of protons. The line width of a resonance at its half-height is approximately proportional to the inverse of the T2 relaxation value of that metabolite. Protons attached to large molecules have a short T2 relaxation time and are observed as a broad, short resonance, whereas protons attached

Teaching Point

to small molecules have longer T2 relaxation times and are observed as narrow, more intense resonances.

Preparing for Spectroscopy

Coils
Most coils currently used for breast MR imaging are multichannel coils. It is important that MR spectroscopy be performed with the same coil used for MR imaging so that the imaging and spectroscopy data are directly comparable. Spectroscopy requires that the raw free induction decay (FID) data collected from each channel be accurately summed prior to Fourier transform. Multichannel coils provide an increased SNR and therefore should be advantageous for in vivo MR spectroscopy (30).

Voxel Prescription
The area of investigation, or region of interest (ROI), is usually chosen after the administration of an MR imaging contrast agent. A breast lesion is identified through a careful consideration of morphology and enhancement kinetics. In prescribing a voxel or voxels for MR spectroscopy, care should be taken to include as much of the lesion as possible while avoiding surrounding adipose tissue. The presence of gadolinium chelates is not thought to adversely affect the performance of breast MR spectroscopy (19).

Pre-acquisition Setup
When undertaking MR spectroscopy, the acquisition parameters are adjusted on a patient-by-patient basis to obtain optimal spectral resolution and SNR. The parameters set during the automated pre-acquisition procedure typically include shimming, power calibrations, frequency adjustment, and water-suppression adjustment. While all the pre-acquisition adjustments are important for obtaining high-quality in vivo MR spectra, shimming and water suppression are particularly important (31). It is crucial to spend the necessary time on these procedures.

Shimming.—In MR spectroscopy, detectable biochemical markers are distinguished from one another by their resonance frequency, line shape, line width, phase, and integral (resonance area) (29,32). The line width of a resonance is dependent both on the intrinsic T2 of the biomarker and the homogeneity of the magnetic field in the region. The line width that is due to the intrinsic T2 is typically less than 1 Hz, whereas the line width from field inhomogeneity may be from 5 to 10 Hz. The term $T2^*$ is used to describe the combined effects of intrinsic T2 and magnetic field inhomogeneity that also contribute to the observed line width. In biologic tissues, several factors can contribute to the inhomogeneity of the magnetic field. Variations in the main magnetic field (B_0) that arise from extrinsic factors (notably, susceptibility-induced field shifts) cause broadening and distortion of these resonance characteristics and must be minimized to acquire high-quality in vivo MR spectral data. Susceptibility-induced magnetic field distortions arise primarily from different magnetic permeabilities, particularly at air–soft tissue interfaces and to a lesser degree at soft tissue–bone interfaces (33). Consequently, when a subject is placed in an MR imaging system, significant B_0 inhomogeneities are generated that depend on the presence and distribution of different tissue types. These B_0 inhomogeneities are often the dominant factor limiting successful MR spectroscopy applications, with in vivo spectroscopy being particularly sensitive to even small variations in magnetic field uniformity.

Because of susceptibility-induced magnetic field inhomogeneities, shimming is usually required for each MR spectroscopy data set (34). Shimming is the process by which the B_0 field is made as homogeneous as possible. This process typically involves adjusting the electric currents in the linear x-, y-, and z-gradient coils used in imaging. Automated shimming, in which a B_0 field map is acquired and the electric current corresponding to each of the available shim coils is adjusted by using a least squares minimization procedure, has greatly improved localized shimming results (35,36). The use of higher-order shim coils capable of generating second- and third-order spherical harmonics, in addition to the shimming of linear gradient coils, also has yielded improved results (37).

While automated shimming procedures provide relatively consistent results in the homogeneous surrounds of the brain, their use for in vivo MR spectroscopy of the breast is more challenging because of the proximity of the lungs and the inherent susceptibility differences between adipose tissue and glandular tissue. It is therefore advisable, after completing the automated shimming procedure, to check the localized shim result and perform any necessary manual adjustments to obtain the highest-quality result for each acquisition (Fig 3). In general, this involves interactive optimization of the water signal (to increase the resonance height and reduce the resonance width) by manually adjusting the electric currents in each of the coils available for shimming individually (Fig 4). This is particularly important at
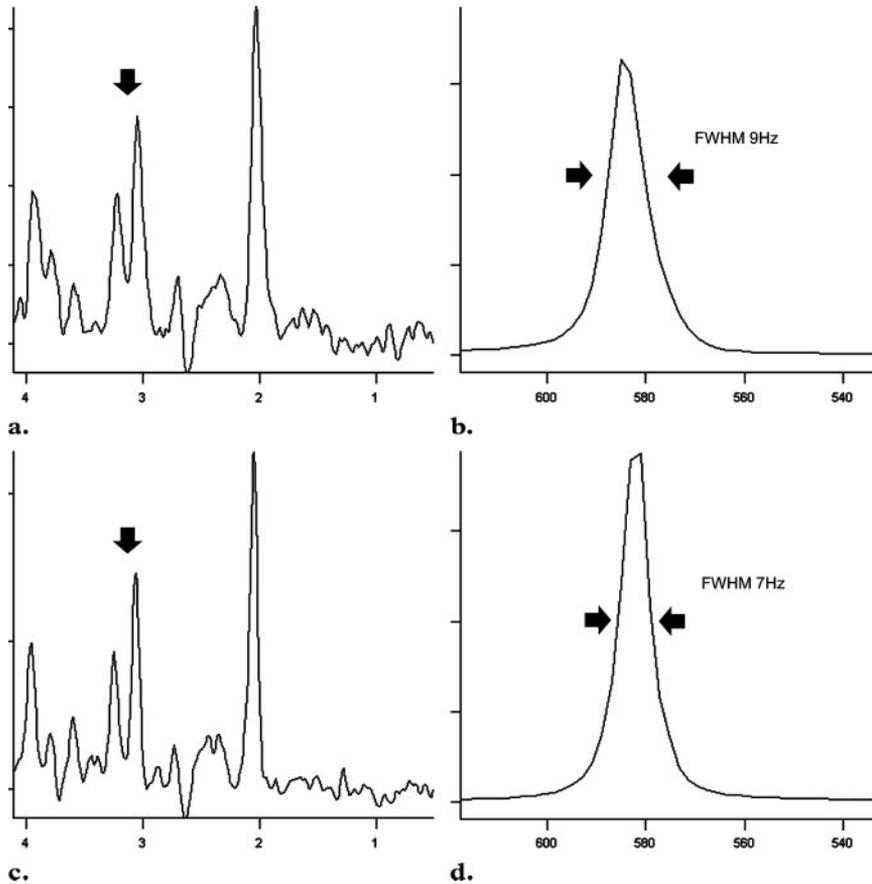
Figure 3. Effect of manual versus automated shimming for optimizing the water signal, demonstrated by using a single-voxel study of a human brain (TR = 2000 msec, TE = 135 msec). **(a)** Spectrum obtained with automated shimming only. The arrow points to the division between the choline and creatine resonances. **(b)** To determine the shim, the unsuppressed water resonance (at 4.74 ppm) is measured. In this case, it has a full width at half maximum (FWHM) of 9 Hz (arrows). **(c)** Spectrum from the same location, obtained with manual shimming. **(d)** The unsuppressed, corresponding water resonance has a FWHM of 7 Hz (arrows). The increased spectral resolution obtained with manual shimming allows for further separation of the resonances at the region indicated by the arrow in **a** and **c**. Spectra were obtained at 3.0 T.
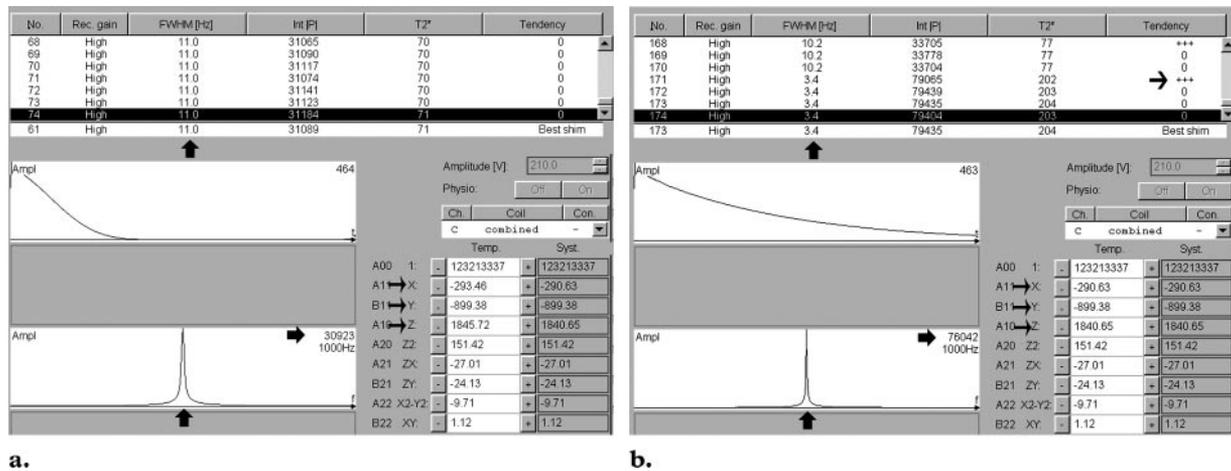

Figure 4. Interactive shimming with the Syngo platform (Siemens; Erlangen, Germany). **(a)** Results obtained with automated prescan conditions: Both vertical arrows show the FWHM to be 11 Hz. The thick horizontal arrow reveals a signal amplitude of 30,923 units. Thin horizontal arrows show the settings of the x-, y-, and z-gradient coils producing this shim. **(b)** Improved results from the same voxel following manual adjustment of the x-, y-, and z-gradient coils (thin horizontal arrows): Vertical arrows show the result of the FWHM of 3.4 Hz. The thick horizontal arrow reveals a signal amplitude of 76,042 units. The thin horizontal arrow in the top panel indicates that the tendency of the interactive adjustment is toward improvement rather than deterioration in the localized shim result. The vertical arrow under the Gaussian water resonance (bottom panel in **a** and **b**) also visually reveals a decrease in the width of the water resonance with improved localized shimming.

higher magnetic field strengths, as susceptibility shifts increase with increasing magnetic field strength. The intricacies of shimming are well covered in a two-part series by Hull (34).

Water Suppression.—For in vivo ^{1}H MR spectroscopy, the water resonance is suppressed to allow the detection of the metabolite signals of
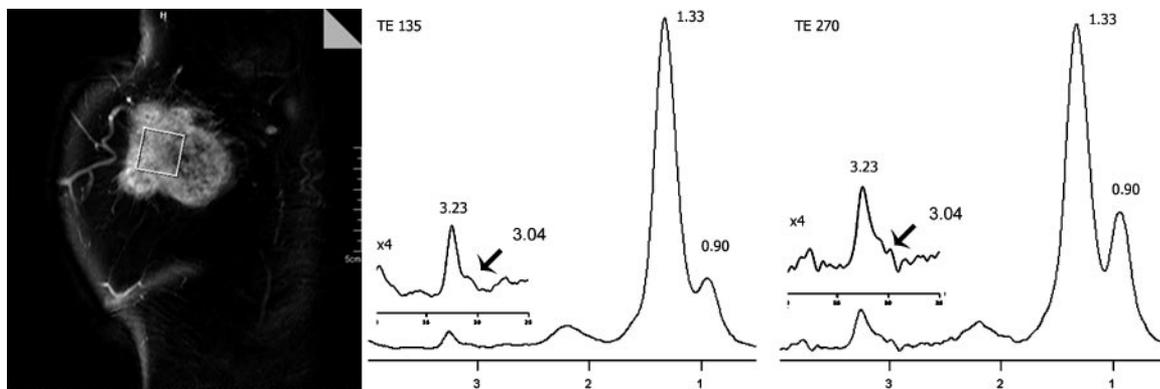
Figure 5.   In the middle and on the right, single-voxel spectra of breast cancer acquired at 3.0 T by using the PRESS sequence. The contrast-enhanced image on the left indicates the voxel placement within a 4-cm invasive ductal carcinoma. The spectrum in the center is a typical water-suppressed spectrum acquired with TR of 2000 msec, TE of 135 msec, and 192 signals acquired. The spectrum on the right was acquired from the same location, with the same TR and the same number of signals acquired, but with TE of 270 msec. Both spectra show resonances at 3.04 ppm from creatine-containing compounds and from phosphocholine at 3.23 ppm. However, the resonance attributable to creatine-containing compounds is better resolved in the spectrum collected with a TE of 270 msec (arrows). This is due to increased T2 relaxation at this longer TE, reducing the amplitude of lipid. It can also be seen that the methyl to methylene resonances (attributable to lipid), at 1.33 and 0.90 ppm, respectively, are reduced in intensity at TE of 270 msec because of increased T2 relaxation of these lipid signals.

interest, which may be 10,000 times less concentrated than the water signal. Water suppression usually involves the implementation of a series of three water-frequency–selective radiofrequency (RF) pulses followed by dephasing gradient pulses that null (flatten) the water signal (38). Because of finite water relaxation times, water suppression is typically achieved by using RF pulse flip angles other than 90° (typically, 110°–120°); thus, improved water suppression may be achieved by varying the flip angle of the final water-frequency–selective RF pulse to null the water signal. Automated pre-acquisition setup procedures include a step in which the flip angle is adjusted to achieve optimal water suppression. The degree of suppression may be further fine-tuned manually by increasing or decreasing the flip angle of the third frequency-selective RF pulse to reduce the amplitude of the water resonance.

Localization and Spectral Data Acquisition

Localization for in vivo MR spectroscopy involves the identification of a spatially dependent ROI for the collection of spectral data without unwanted signal from surrounding tissues. For in vivo studies a voxel size of 3– 8 cm^3 generally is used; however, with current higher-field-strength MR imaging systems, a voxel as small as 1 cm^3 may be selected. The smaller the voxel, the smaller the amount of tissue present within it; hence, there

may be a need to improve the SNR by increasing the examination time. Thus, there is a trade-off between the size of the voxel and the acquisition time.

The two commonly used localization methods are single-voxel spectroscopy (SVS) and spectroscopic imaging (SI).

Localization with SVS

SVS makes use of modulated, frequency-selective RF pulses applied in the presence of a pulsed gradient field to select the volume for spectral measurement (a single voxel) (Fig 5). Three selective pulses are applied, one after the other, in the presence of mutually orthogonal field gradients (39). The intersections of the three planes define the ROI.

Localization with SI

Within the same acquisition time as that required for spectral measurement of a single voxel with SVS, SI may be performed to collect an array of spectra from a two-dimensional plane or three-dimensional volume containing multiple voxels (42). Phase-encoding gradients are employed to encode the spatial dimensions, and the MR signal is collected in the absence of any gradient, to maintain the spectroscopic information. A separate MR spectrum is collected from each voxel; thus, the metabolic profile of tissue in the individual voxel locations can be inspected, as can the spatial distribution of specific metabolites of interest across multiple voxels (Fig 6). SI also allows data acquisition from a smaller voxel (as small as 0.8 cm^3 at higher magnetic field
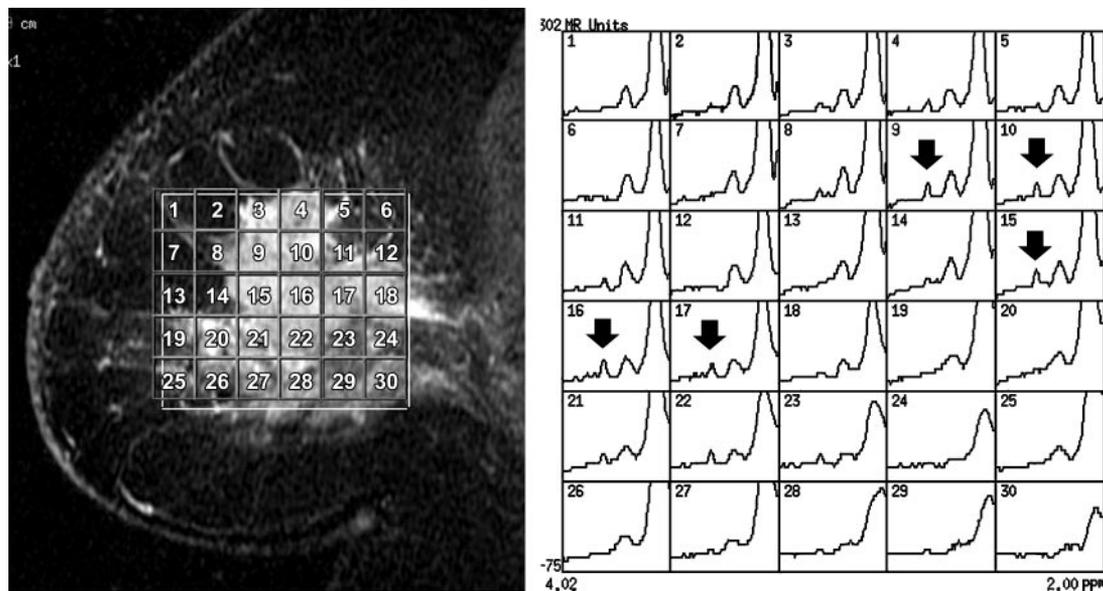
Figure 6. The sagittal image on the left (TR = 4000 msec, TE = 70 msec, TI = 150 msec) indicates the location of an acquisition array positioned within an area of breast cancer. The figure on the right shows an array of spectra from SI, acquired at 1.5 T by using the PRESS sequence (TR = 1150 msec, TE = 135 msec). All spectra are within the spectral region of 2–4 ppm. Each numbered spectrum in this array corresponds to a voxel with the same number superimposed on the image. The tCho resonance at 3.2 ppm is seen in the voxels that correspond to the spatial distribution of cancer (voxels 4, 8, 9, 10, 11, 14, 15, 16, 17, 21, 22, 23, 27, 28, and 29) and is most prominent in voxels 9, 10, and 15–17, where the resonance is indicated by the arrow.

strengths) than is possible with SVS. However, SI has the disadvantage that the voxel shape may be less well defined than with SVS. This can result in the contamination of spectral data from individual voxels by large-amplitude signals emanating from surrounding voxels. Although SI with a smaller voxel size may be more time consuming than SVS, SI may be used to examine a larger area. Efforts to reduce the acquisition time for SI are under development (43,44).

Acquisition Techniques

Two commonly used techniques for localization and interrogation of a voxel or voxels are stimulated echo acquisition mode (STEAM) (40) and point-resolved spatially localized spectroscopy (PRESS) (41).

STEAM Technique.—The sensitive volume in STEAM localization is selected by applying three consecutive frequency-selective 90° pulses to generate a stimulated echo from the ROI; full localization is achieved in a single acquisition, and there is no need for phase cycling (40). Advantages of the STEAM technique include a well-delineated ROI, because the frequency-selective 90° pulses generate a good section profile. In addition, signal losses due to T2 relaxation remain minor. There is excellent water suppression, and the 90° RF pulses employed are more broadband than equivalent 180° pulses, with the advantage

that the resultant localized signal is less dependent on RF inhomogeneities. However, with the use of STEAM localization, there may be a signal loss of up to 50%, in comparison with the PRESS technique; this signal decrease may translate into an increase of up to 26% in the voxel dimension or a fourfold increase in acquisition time (39). Figure 1 is an example of breast MR spectroscopy data collected by using STEAM.

PRESS Technique.—The sensitive volume in PRESS localization is selected by applying a frequency-selective 90° pulse followed by two frequency-selective 180° pulses to generate a spin echo from the ROI (41). The principal advantage of PRESS over STEAM is the additional gain in SNR with the collection of a spin echo as opposed to a stimulated echo. However, T2 losses are more pronounced with PRESS than with STEAM, and the SNR advantage gained with PRESS may be partially reduced if the T2 losses are significant. Disadvantages of PRESS include a poor section profile even if improved pulse designs are employed. Moreover, the transition bands of the RF pulses generate unwanted coherences that need to be eliminated. In addition, maximum RF power is required to retain the same chemical shift displacement error with PRESS when compared to STEAM. Typical
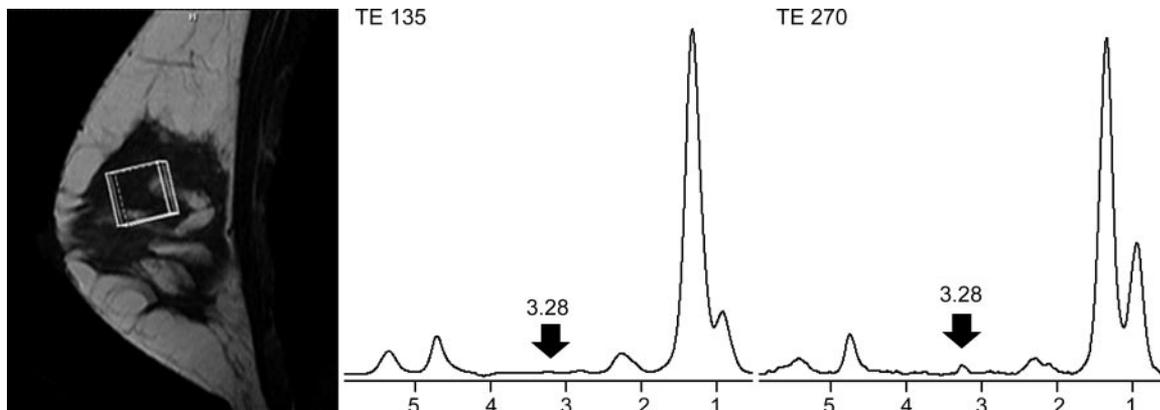
Teaching Point

Teaching Point

Figure 7.   Single-voxel spectra in the middle and on the right, acquired at 3.0 T by using the PRESS sequence, from an apparently healthy volunteer. The image on the left indicates the voxel placement within the glandular tissue. In the center there is a typical water-suppressed spectrum acquired with TR of 2000 msec, TE of 135 msec, and 192 signals acquired. The spectrum on the right is acquired from the same location, with the same TR but with TE of 270 msec. There is a resonance centered at 3.28 ppm in both spectra. Increasing the TE from 135 to 270 msec reduces the amplitude of lipid (at 0.90 and 1.33 ppm) due to increased T2 relaxation, and as a consequence the resonance at 3.28 ppm is more prominent at the longer TE. Note that if this 3.28 ppm resonance were interpreted as a broad composite resonance in the 3.2 ppm region it would be a false-positive.

single-voxel spectra obtained with a PRESS sequence and with TEs of 135 msec and 270 msec are shown in Figure 7.

Pitfalls in Data Acquisition

The in vivo ^{1}H MR spectra from the breast are often dominated by lipid resonances. When adipose tissue that is not part of the pathologic process in breast cancer is included in the ROI for MR spectroscopy, its inclusion causes several problems. Adipose tissue makes localized shimming more difficult because its magnetic susceptibility differs from that of surrounding glandular (and malignant) tissues. In addition, the interaction between lipid signals and the pulsed gradients necessary for localization may produce lipid sideband artifacts, which may produce spectral artifacts that hinder interpretation (45). With in vivo MR spectroscopy, the amplitude of these artifacts may be as large as the amplitude of the resonances in the 3–4-ppm region. However, the effects of unwanted lipid signals can be reduced by using various techniques to decrease the lipid signal amplitude.

Techniques for limiting the effects of unwanted lipid signals include suppression of the signal either through the application of an inversion-recovery technique or by selective frequency suppression of the dominant lipid signal. However, suppression of the lipid resonance eliminates the possibility of assessing lipid that actually is involved in the disease process. Similarly, a

method has been proposed in which spectral data are collected from the same volume by using several different TEs, a technique that results in coherent cancellation of the sideband artifacts (45).

A less complicated method for limiting the effects of unwanted lipid signal is the careful placement of the spectroscopic ROI. For this reason, the voxel selection is best planned on the basis of early-phase contrast-enhanced imaging in conjunction with non–fat-saturated imaging. Dynamic contrast-enhanced imaging allows the identification of an enhancing lesion before the noninvolved breast parenchyma enhances, while non–fat-saturated imaging allows the determination of the spatial distribution of noninvolved adipose tissue. In addition, the use of a long TE (135–350 msec) has been advocated to reduce the amplitude of the lipid and water signals through natural T2 relaxation effects that still allow the assessment of pathophysiologic lipid signals (22) (Fig 5).

Quantitative MR Spectroscopy

Quantitation of the recorded tCho signal has been advocated as an indicator of breast malignancy (21). Only molecules that are mobile on the MR timescale are available for inspection with MR spectroscopy. However, the rationale for quantitation is that the area of the resonance is proportional to the number of protons contributing to the signal. Thus, the number of molecules measurable by MR spectroscopy may be derived from the calculated integral (resonance area) for that compound or may be expressed as a ratio of another resonance or standard.
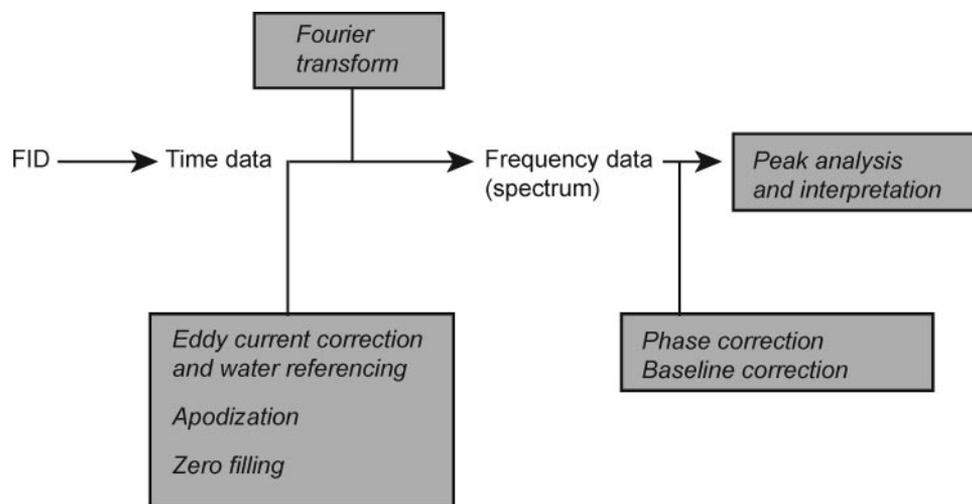
Figure 8. Flow scheme for processing of a raw time-domain data file from MR spectroscopy, from collection of the FID signal to clinical diagnosis. The raw data may be processed by software supplied by MR system manufacturers or by stand-alone software.

There are two common approaches to quantitation: Intravoxel water may be used as an internal reference (21), or an external standard may be chosen (46). However, for accurate measurement of the relative amount of a metabolite, the resonance must be corrected for by the relaxation properties of the signal and optimally must not overlap with any other resonances in the spectrum. That is often difficult to accomplish when low signal intensity is encountered, as is often the case in spectroscopy performed at the commonly used field strength of 1.5 T.

Postprocessing

The postprocessing of the FID signal through a Fourier transform is essential for the interpretation of proton MR spectroscopy data. Several important steps are required to compensate for any introduced artifacts (eg, eddy currents) and to optimize spectral analysis (eg, increase spectral resolution and calculate the resonance integral). While the optimization of acquisition techniques is key for the collection of high-quality ^{1}H MR spectral data, important spectral information also may be obtained through the optimal postprocessing of data, particularly data acquired in vivo, in the clinical setting (Fig 8).

During data collection, the FID signal is converted from analog to digital format. The resolution of the resultant digital signal determines the spectral resolution. After data collection, MR signal postprocessing is performed. The processing steps that are usually applied to the time-domain data consist of water referencing, apodization, and zero filling (Fig 8). Then, after the Fourier transform and before the spectral resonance analysis and interpretation, a phase correction and baseline correction are performed on the frequency-domain data. These crucial steps in the postprocessing of in vivo breast spectra are described below and in Figure 2.

Eddy Current Correction and Water Referencing

Rapid alternations in polarity of the gradient magnetic field may produce electric currents known as eddy currents in the conductive structures that surround the magnet. In the absence of any compensation or correction measures, these eddy currents produce time-dependent shifts of the resonance frequency, which result in distortion of the spectrum after Fourier transform. Most modern MR imaging systems are equipped with actively shielded gradients that minimize the effect of eddy currents. If necessary, a correction may be performed by using the water signal collected without water suppression as a reference. Careful use of the water signal as a reference to correct for frequency variations may help to accurately determine the exact frequency of any detected resonance in the 3.00–3.50-ppm spectral region (47). Careful referencing of the spectrum has proved to be important for distinguishing between normal and malignant breast tissue (20).

Apodization

Apodization is the multiplication of the raw MR time-domain signal by a particular function with the intention of improving the SNR and spectral resolution, removing truncation artifacts, or removing broad spectral components in the frequency domain (48). For MR spectroscopy in vivo, the most common filter functions decay with time, so the signal is enhanced at the beginning of the data collection period and is suppressed at the end (Fig 9). In addition, the center of a filter
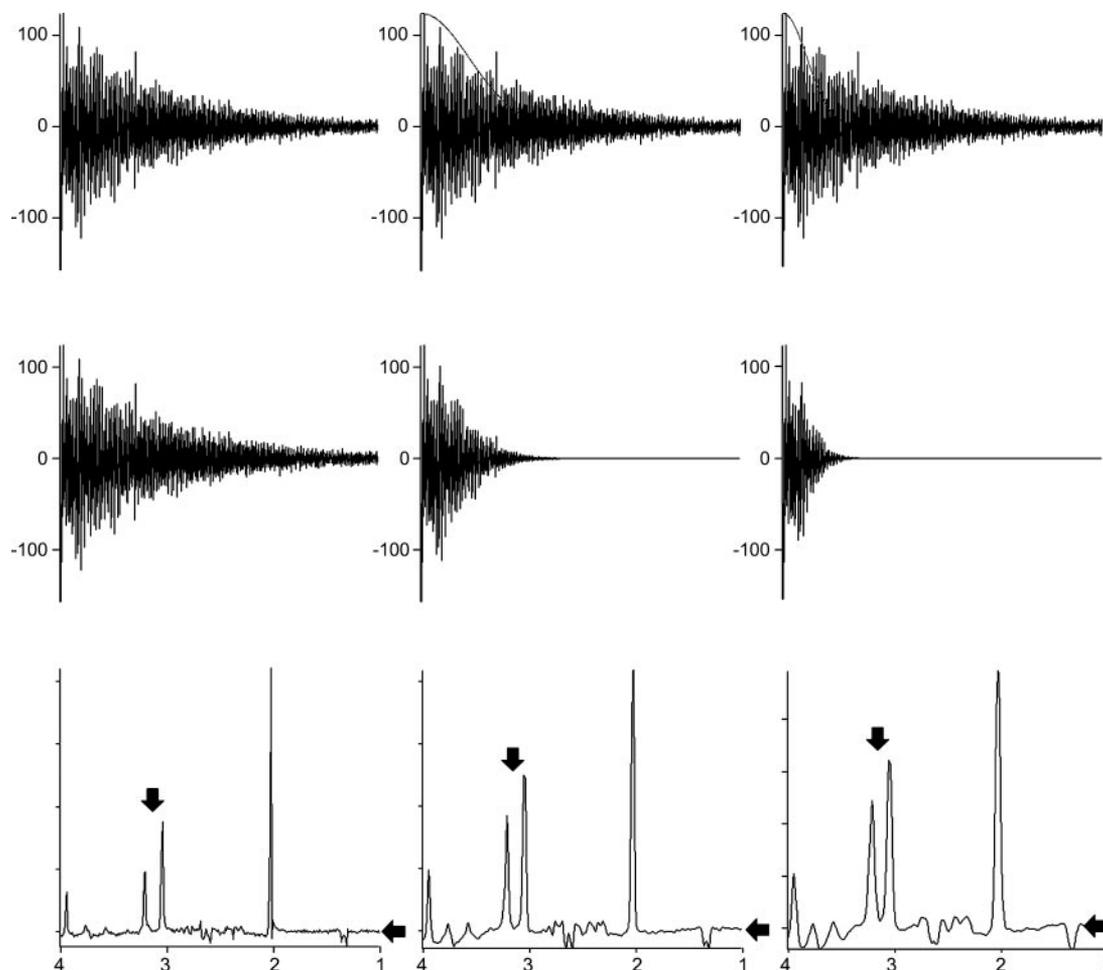
Figure 9.   The effect of time-domain data apodization (postprocessing of the FID signal) with the application of different decay filter functions. The top row shows the data prior to processing. The middle row shows the effect of each of the following filter functions: no filter (left column), a 300-msec filter (middle column), and a 150-msec filter (right column). The bottom row shows the product of this postprocessing, after Fourier transform. In this last row, two trends are evident from left to right: the SNR can be seen to improve, visualized as loss of the noise ripple (horizontal arrows), whereas spectral resolution declines, visualized as the decreased separation of the two resonances at approximately 3.0–3.3 ppm (vertical arrows).

function may be shifted in such a way that it coincides with the part of the FID signal that requires the most enhancement (echo offset). Note that apodization may alter relative resonance intensities and therefore should be applied carefully. In addition, the specific details of the process should be described accurately when results are reported.

Zero Filling

Zero filling is a method of artificially increasing the number of digital data points by inserting additional data points of zero amplitude at the end of the FID, following data acquisition. Zero filling of the time-domain signal data achieves the same effect as interpolation of the frequency-domain signal data. This method helps improve spectral resolution by producing a better representation of

Figure 10.   The effect of zero filling on spectral resolution. Spectra in *A* and *B* both were treated with a Gaussian apodization function of 1.5 Hz and a 15% echo offset. *A* was zero filled from 1024 to 2048 data points, while *B* was not. Fourier transform was then performed on each. Spectral resolution is improved, as shown by the evidence of finer details in *A*. The arrows denote resonances that were not resolved in the data set without zero filling.
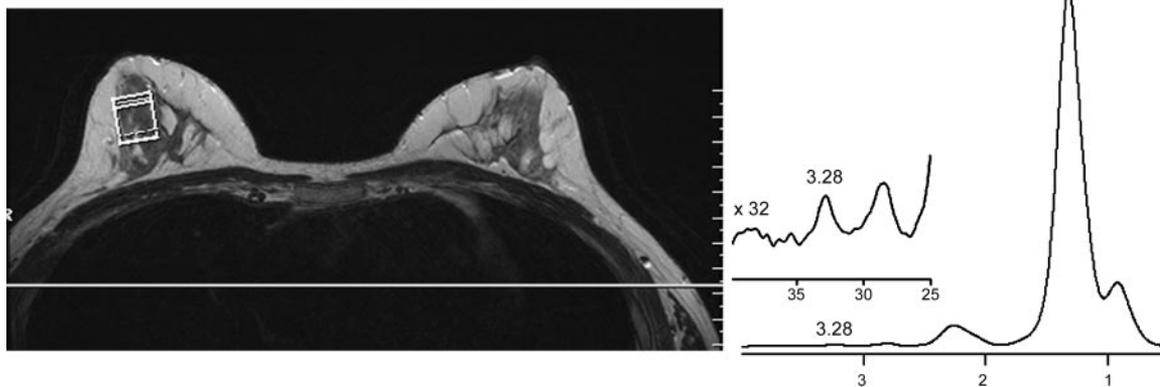
Figure 11.   The axial T2-weighted image on the left indicates the voxel placement within the glandular tissue in a healthy volunteer. The single-voxel spectrum on the bottom right was acquired at 3.0 T by using the PRESS sequence (TR = 2000 msec, TE = 135 msec, 192 signals acquired) and is typical of water-suppressed spectra acquired with this sequence. There is no discernible resonance at 3.2 ppm. When the vertical display is increased and the spectral region of 2.00–4.00 ppm is displayed (inset above), a discrete resonance is seen at 3.28 ppm. Note that if this 3.28 ppm resonance were interpreted as a broad composite resonance in the 3.2 ppm region, this would have been a false-positive.

fine details, allowing a more accurate definition of the position and height of resonances, and, hence, evaluation of the relative amounts of metabolites (Fig 10) (49).

Phase Correction

During a spectroscopy measurement, phase shifts may be introduced as a result of hardware settings, sequence timing (which produces frequency-dependent phase shifts), or both. Following the Fourier transform, these shifts introduce a mixture of absorption and dispersion signals into the frequency spectrum. Since final interpretation is performed on a pure absorption spectrum, phase correction is required to separate pure absorption and pure dispersion modes into the real and imaginary parts of the complex spectrum.

Baseline Correction

The baseline of an MR spectrum should be flat until the resonance is reached; however, several factors may affect the baseline. These include a delay between RF excitation and the beginning of the FID signal collection, a factor that may produce a rolling baseline even after appropriate phase correction. This may occur during proton SI, when time is allowed for phase encoding before FID signal collection. Other baseline distortions may be due to broad spectral humps from compounds such as macromolecules with a short T2 (50).

Resonance Assignment

The identification and assignment of metabolites in spectra from in vivo proton MR spectroscopy of the breast may be accomplished in several ways. First, spectra may be acquired by using phantoms that contain known concentrations of compounds thought to be present in the pathologic processes under investigation by using the same experimental parameters. Large databases of MR spectral resonances, frequencies, intensities, and other parameters for known compounds have been accumulated over the past 30 years and are available to assist in this process of metabolite identification (51). Second, spectra may be obtained with different TEs to observe the behavior of the resonances at different TEs. This method provides information about the T2 values of the resonances and may reveal resonance multiplicity (51). Third, more-sophisticated MR experiments, such as "editing" and two-dimensional correlated spectroscopy, may be performed in vivo to assist in the assignment of resonances to specific molecules (52,53).

What We Can Expect When Using the Protocol Described

The goal is to devise acquisition and postprocessing techniques that will allow the most effective use of in vivo ^{1}H MR spectroscopy for noninvasive preoperative identification and diagnosis of breast lesions. The hypothesis that a malignancy may be diagnosed confidently on the basis of the detection of a broad composite choline resonance at in vivo proton MR spectroscopy has been challenged. Current efforts are concentrated on recognizing the frequencies of detected signals in the 3–4-ppm region and quantifying those resonances. There is a need for consistently high spectral quality, sufficient SNR, and sufficient spectral resolution to allow the separation of resonances in the 3–4-ppm region and, thus, to distinguish lesions with abnormal biochemical activity but without malignant disease (Fig 11).

For patients with lesions identified at previous imaging with other modalities, once the quality criteria described above are implemented, spectra can be collected with sufficient SNR to enable distinction of a malignancy, a benign lesion, and normal breast tissue on the basis of resonances at discrete frequencies. The difference between the spectral resonances indicative of a malignancy and those indicative of a benign lesion is clearly visible in Figure 12. The spectrum obtained in a breast carcinoma has a resonance at 3.23 ppm, which is representative of phosphocholine, whereas the spectrum obtained in a fibroadenoma has a resonance at the frequency of 3.28 ppm due to differences in the biochemical contents of the nonmalignant tissue (eg, in the individual or combined levels of glycerophosphocholine, taurine, or myoinositol).

Teaching Point

Data acquisition and spectral interpretation based on this frequency difference have been successfully performed in many patients at 3.0 T by using a commercially available MR imaging system (Trio; Siemens) and a four-channel breast coil (InVivo, Orlando, Fla). This MR imaging system has capabilities for interactive manual adjustment of the pre-acquisition parameters (shimming and water suppression) and is equipped with the software required for the adding of data from individual coil elements and for postprocessing and display of the final spectra. For other manufacturers, the capabilities are dependent on the model.

Just how small a lesion can be measured by this method has yet to be tested; at present, lesions of 1 cm^3 are routinely examined. The very basis of the spectroscopy method relies on the use of magnets with higher field strength to separate the diagnostic resonances. In addition, the higher the field strength, the smaller the voxel size achievable. A 3.0-T system with the hardware and software described should be capable of producing spectra of the quality shown in this article within 6 minutes. However, at present, in vivo spectroscopy of the breast is operator dependent and manufacturer dependent. The examples of spectra included in this article were obtained by a spectroscopist who also recorded the shim value and SNR with each data acquisition, to facilitate subsequent comparisons of spectral quality.
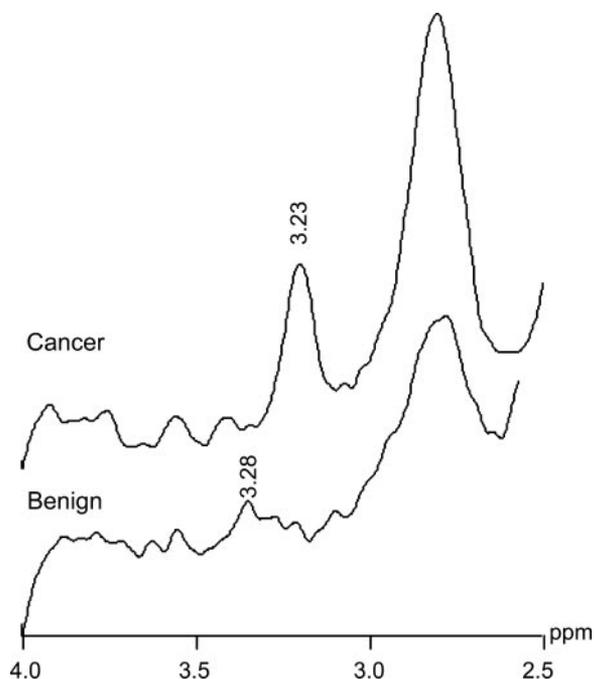

Figure 12. In vivo breast single-voxel spectra obtained at 3.0 T by using the PRESS sequence (TR = 2000 msec, TE = 135 msec; 192 signals acquired). The spectra were processed as described in Figure 2 and were referenced to the methylene resonance of lipid at 1.33 ppm and water at 4.74 ppm. The top spectrum is from an infiltrating ductal carcinoma. The bottom spectrum is from a fibroadenoma. In the spectrum from the cancer, the resonance is at 3.23 ppm and is consistent with phosphocholine. In the spectrum from the fibroadenoma, the resonance is centered at 3.28 ppm. These differences allow a distinction between the disease states.

Conclusions

In vivo proton MR spectroscopy can be applied successfully in the breast, preoperatively and noninvasively, to distinguish malignancies from benign lesions and healthy tissue with a high level of accuracy. For successful application, the method relies on access to the following tools:

1. Coils that generate adequate SNR and cover the breast adequately.

2. An MR imaging system that facilitates the pre-acquisition setup (interactive shimming and interactive adjustment of water suppression) to ensure adequate SNR and spectral resolution.

3. Higher-order shim coils to achieve acceptable localized shim results at higher magnetic field strengths.

RadioGraphics

4. The capacity to add data from separate channels of a multichannel array coil.

5. Flexibility in postprocessing software, or the ability to transfer data to a stand-alone postprocessing system.

The Future

The future will see improved sensitivity with increased SNR through the further development of specialized coils. There will be an increase in the use of magnets with higher field strength, which is important for high-quality spectroscopy because increased field strength yields increased spectral resolution. New and improved pulse sequences for in vivo spectroscopy will allow faster data acquisition, and two-dimensional spectroscopic imaging will allow mapping of the spatial distribution of disease.

In the meantime, the use of MR-guided biopsy devices will facilitate the correlation of MR spectroscopy results with histopathologic findings by allowing the collection of biopsy material from the exact location interrogated during spectroscopy. This will allow the in vivo spectroscopic diagnosis to be confirmed unambiguously by examining the precise piece of tissue with correlative histopathology.

References

1. Lehman CD, Gatsonis C, Kuhl CK, et al. MRI evaluation of the contralateral breast in women with recently diagnosed breast cancer. N Engl J Med 2007;356:1295–1303.
2. Saslow D, Boetes C, Burke W, et al. American Cancer Society guidelines for breast screening with MRI as an adjunct to mammography. CA Cancer J Clin 2007;57:75–89.
3. Mountford CE, Doran S, Lean CL, Russell P. Proton MRS can determine the pathology of human cancers with a high level of accuracy. Chem Rev 2004;104:3677–3704.
4. Mountford C, Lean C, Malycha P, Russell P. Spectroscopy provides accurate pathology on biopsy and in vivo. J Magn Reson Imaging 2006;24:459–477.
5. Lean C, Doran S, Somorjai RL, et al. Determination of grade and receptor status from the primary breast lesion by magnetic resonance spectroscopy. Technol Cancer Res Treat 2004;3:551–556.
6. Mountford CE, Somorjai RL, Malycha P, et al. Diagnosis and prognosis of breast cancer by magnetic resonance spectroscopy of fine-needle aspirates analysed using a statistical classification strategy. Br J Surg 2001;88:1234–1240.
7. Ackerstaff E, Glunde K, Bhujwalla ZM. Choline phospholipid metabolism: a target in cancer cells? J Cell Biochem 2003;90:525–533.
8. Glunde K, Jie C, Bhujwalla ZM. Molecular causes of the aberrant choline phospholipid metabolism in breast cancer. Cancer Res 2004;64:4270–4276.
9. Katz-Brull R, Lavin P, Lenkinski RE. Clinical utility of proton magnetic resonance spectroscopy in characterizing breast lesions. J Natl Cancer Inst 2002;94:1197–1203.
10. Podo F. Tumour phospholipid metabolism. NMR Biomed 1999;12:413–439.
11. Aboagye EO, Bhujwalla ZM. Malignant transformation alters membrane choline phospholipid metabolism of human mammary epithelial cells. Cancer Res 1999;59:80–84.
12. Sitter B, Sonnewald U, Spraul M, Fjosne HE, Gribbestad IS. High-resolution magic angle spinning MRS of breast cancer tissue. NMR Biomed 2002;15:327–337.
13. Roebuck JR, Cecil KM, Schnall MD, Lenkinski RE. Human breast lesions: characterization with proton MR spectroscopy. Radiology 1998;209:269–275.
14. Sharma U, Jagannathan NR. In vivo magnetic resonance spectroscopy in breast cancer. Amsterdam, the Netherlands: Springer, 2007.
15. Cecil KM, Schnall MD, Siegelman ES, Lenkinski RE. The evaluation of human breast lesions with magnetic resonance imaging and proton magnetic resonance spectroscopy. Breast Cancer Res Treat 2001;68:45–54.
16. Gribbestad IS, Singstad TE, Nilsen G, et al. In vivo 1H MRS of normal breast and breast tumors using a dedicated double breast coil. J Magn Reson Imaging 1998;8:1191–1197.
17. Jacobs MA, Barker PB, Bottomley PA, Bhujwalla Z, Bluemke DA. Proton MR spectroscopic imaging of human breast cancer: a preliminary study. J Magn Reson Imaging 2004;19:68–75.
18. Jagannathan NR, Kumar M, Seenu V, et al. Evaluation of total choline from in-vivo volume localized proton MR spectroscopy and its response to neoadjuvant chemotherapy in locally advanced breast cancer. Br J Cancer 2001;84:1016–1022.
19. Yeung DK, Cheung HS, Tse GM. Human breast lesions: characterization with contrast-enhanced in vivo proton MR spectroscopy—initial results. Radiology 2001;220:40–46.
20. Stanwell P, Gluch L, Clark D, et al. Specificity of choline metabolites for in vivo diagnosis of breast cancer using 1H MRS at 1.5 T. Eur Radiol 2005;15:1037–1043.
21. Bolan PJ, Meisamy S, Baker EH, et al. In vivo quantification of choline compounds in the breast with 1H MR spectroscopy. Magn Reson Med 2003;50:1134–1143.

22. Kvistad KA, Bakken IJ, Gribbestad IS, et al. Characterization of neoplastic and normal human breast tissues with in vivo 1H MR spectroscopy. J Magn Reson Imaging 1999;10:159–164.

23. Tomanek B, Hoult DI, Chen X, Gordon R. Probe with chest shielding for improved breast MRI. Magn Reson Med 2000;43:917–920.

24. Bartella L, Morris EA, Dershaw DD, et al. Proton MR spectroscopy with choline peak as malignancy marker improves positive predictive value for breast cancer diagnosis: preliminary study. Radiology 2006;239:686–692.

25. Kumar M, Jagannathan NR, Seenu V, Dwivedi SN, Julka PK, Rath GK. Monitoring the therapeutic response of locally advanced breast cancer patients: sequential in vivo proton MR spectroscopy study. J Magn Reson Imaging 2006;24:325–332.

26. Meisamy S, Bolan PJ, Baker EH, et al. Neoadjuvant chemotherapy of locally advanced breast cancer: predicting response with in vivo 1H MR spectroscopy—a pilot study at 4 T. Radiology 2004;233:424–431.

27. Meisamy S, Bolan PJ, Baker EH, et al. Adding in vivo quantitative 1H MR spectroscopy to improve diagnostic accuracy of breast MR imaging: preliminary results of observer performance study at 4.0 T. Radiology 2005;236:465–475.

28. Tse GM, Cheung HS, Pang LM, et al. Characterization of lesions of the breast with proton MR spectroscopy: comparison of carcinomas, benign lesions, and phyllodes tumors. AJR Am J Roentgenol 2003;181:1267–1272.

29. de Graaf R. In vivo NMR spectroscopy: principles and techniques. Chichester, England: Wiley, 1998.

30. Wright SM, Wald LL. Theory and application of array coils in NMR spectroscopy. NMR Biomed 1997;10:394–410.

31. Kreis R. Quantitative localized 1H MR spectroscopy for clinical use. Prog Nucl Magn Reson Spectrosc 1997;31:155–195.

32. Gadian DG. NMR and its applications to living systems. Oxford, England: Oxford University Press, 1995.

33. Edelman RR, Hesselink JR, Zlatkin MB, Crues JV, eds. Clinical magnetic resonance imaging. Philadelphia, Pa: Saunders-Elsevier, 2005.

34. Hull WE. Computerized shimming with the simplex algorithm. Bruker Spin Rep 2003;154:15–17.

35. Gruetter R. Automatic, localized in vivo adjustment of all first- and second-order shim coils. Magn Reson Med 1993;29:804–811.

36. Kanayama S, Kuhara S, Satoh K. In vivo rapid magnetic field measurement and shimming using single scan differential phase mapping. Magn Reson Med 1996;36:637–642.

37. Spielman DM, Adalsteinsson E, Lim KO. Quantitative assessment of improved homogeneity using higher-order shims for spectroscopic imaging of the brain. Magn Reson Med 1998;40:376–382.

38. Haase A, Frahm J, Hanicke W, Matthaei D. 1H NMR chemical shift selective (CHESS) imaging. Phys Med Biol 1985;30:341–344.

39. von Kienlin M. Single voxel methods and spectroscopic imaging [abstr]. In: Proceedings of the Twelfth Meeting of the International Society for Magnetic Resonance in Medicine. Berkeley, Calif: International Society for Magnetic Resonance in Medicine, 2004.

40. Frahm J, Merboldt KD, Hanicke W. Localized proton spectroscopy using stimulated echoes. J Magn Reson 1987;72:502–508.

41. Bottomley PA. Spatial localization in NMR spectroscopy in vivo. Ann N Y Acad Sci 1987;508:333–348.

42. Maudsley AA, Hilal SK, Perman WH, Simon HE. Spatially resolved high resolution spectroscopy by four-dimensional NMR. J Magn Reson 1983;51:147–152.

43. Dydak U, Pruessmann KP, Weiger M, Tsao J, Meier D, Boesiger P. Parallel spectroscopic imaging with spin-echo trains. Magn Reson Med 2003;50:196–200.

44. Maudsley AA, Matson GB, Hugg JW, Weiner MW. Reduced phase encoding in spectroscopic imaging. Magn Reson Med 1994;31:645–651.

45. Bolan PJ, DelaBarre L, Baker EH, et al. Eliminating spurious lipid sidebands in 1H MRS of breast lesions. Magn Reson Med 2002;48:215–222.

46. Bakken IJ, Gribbestad IS, Singstad TE, Kvistad KA. External standard method for the in vivo quantification of choline-containing compounds in breast tumors by proton MR spectroscopy at 1.5 Tesla. Magn Reson Med 2001;46:189–192.

47. de Beer R, van den Boogaart A, van Ormondt D, et al. Application of time-domain fitting in the quantification of in vivo 1H spectroscopic imaging data sets. NMR Biomed 1992;5:171–178.

48. in 't Zandt H, van der Graaf M, Heerschap A. Common processing of in vivo MR spectra. NMR Biomed 2001;14:224–232.

49. Freeman R. A handbook of nuclear magnetic resonance. Harlow, England: Longman, 1997.

50. Salibi N, Brown MA. Clinical MR spectroscopy: first principles. New York, NY: Wiley-Liss, 1998.

51. Govindaraju V, Young K, Maudsley AA. Proton NMR chemical shifts and coupling constants for brain metabolites. NMR Biomed 2000;13:129–153.

52. Thomas MA, Yue K, Binesh N, et al. Localized two-dimensional shift correlated MR spectroscopy of human brain. Magn Reson Med 2001;46:58–67.

53. Thomas MA, Chung HK, Middlekauff H. Localized two-dimensional 1H magnetic resonance exchange spectroscopy: a preliminary evaluation in human muscle. Magn Reson Med 2005;53:495–502.

In Vivo Proton MR Spectroscopy of the Breast

Peter Stanwell, PhD and Carolyn Mountford, DPhil

Page S255

This article describes a method for obtaining in vivo MR spectra from the breast, in as short a time as possible, with a signal-to-noise ratio (SNR) sufficient to allow the diagnostic resonances to be recorded, while maintaining the highest possible spectral resolution. Success depends greatly on the capability of the MR imaging system to operate as a spectrometer.

Page S256

While all the pre-acquisition adjustments are important for obtaining high-quality in vivo MR spectra, shimming and water suppression are particularly important. It is crucial to spend the necessary time on these procedures.

Page S259

Two commonly used techniques for localization and interrogation of a voxel or voxels are stimulated echo acquisition mode (STEAM) and point-resolved spatially localized spectroscopy (PRESS). The sensitive volume in STEAM localization is selected by applying three consecutive frequency-selective 90° pulses to generate a stimulated echo from the ROI; full localization is achieved in a single acquisition, and there is no need for phase cycling. Advantages of the STEAM technique include a well-delineated ROI, because the frequency-selective 90° pulses generate a good section profile. In addition, signal losses due to T2 relaxation remain minor.

Page S259

The sensitive volume in PRESS localization is selected by applying a frequency-selective 90° pulse followed by two frequency-selective 180° pulses to generate a spin echo from the ROI. The principal advantage of PRESS over STEAM is the additional gain in SNR with the collection of a spin echo as opposed to a stimulated echo. However, T2 losses are more pronounced with PRESS than with STEAM, and the SNR advantage gained with PRESS may be partially reduced if the T2 losses are significant.

Page S264

The spectrum obtained in a breast carcinoma has a resonance at 3.23 ppm, which is representative of phosphocholine, whereas the spectrum obtained in a fibroadenoma has a resonance at the frequency of 3.28 ppm due to differences in the biochemical contents of the nonmalignant tissue (eg, in the individual or combined levels of glycerophosphocholine, taurine, or myoinositol).